

---

# Functional Indirection Neural Estimator for Better Out-of-distribution Generalization

---

Kha Pham<sup>1</sup> Hung Le<sup>1</sup> Man Ngo<sup>2</sup> Truyen Tran<sup>1</sup>

<sup>1</sup> Applied Artificial Intelligence Institute, Deakin University

<sup>2</sup> Faculty of Mathematics and Computer Science, VNUHCM-University of Science

<sup>1</sup> {phti, thai.le, truyen.tran}@deakin.edu.au

<sup>2</sup> nmman@hcmus.edu.vn

## Abstract

The capacity to achieve out-of-distribution (OOD) generalization is a hallmark of human intelligence and yet remains out of reach for machines. This remarkable capability has been attributed to our abilities to make conceptual abstraction and analogy, and to a mechanism known as indirection, which binds two representations and uses one representation to refer to the other. Inspired by these mechanisms, we hypothesize that OOD generalization may be achieved by performing analogy-making and indirection in the *functional* space instead of the data space as in current methods. To realize this, we design FINE (Functional Indirection Neural Estimator), a neural framework that *learns to compose functions* that map data input to output on-the-fly. FINE consists of a backbone network and a trainable semantic memory of basis weight matrices. Upon seeing a new input-output data pair, FINE dynamically constructs the backbone weights by mixing the basis weights. The mixing coefficients are indirectly computed through querying a separate corresponding semantic memory using the data pair. We demonstrate empirically that FINE can strongly improve out-of-distribution generalization on IQ tasks that involve geometric transformations. In particular, we train FINE and competing models on IQ tasks using images from the MNIST, Omniglot and CIFAR100 datasets and test on tasks with unseen image classes from one or different datasets and unseen transformation rules. FINE not only achieves the best performance on all tasks but also is able to adapt to small-scale data scenarios.

## 1 Introduction

*Every computer science problem can be solved with a higher level of indirection.*

—Andrew Koenig, Butler Lampson, David J. Wheeler

Generalizing to new circumstances is a hallmark of intelligence [16, 4, 11]. In some Intelligence Quotient (IQ) tests—a popular benchmark for human intelligence—one must leverage their prior experience to identify the hidden abstract rules out of a concrete example (e.g., a transformation of an image) and then apply the rules to the next (e.g., a new set of images of totally different appearance). These tasks necessitate several key capabilities, including conceptual *abstraction* and *analogy-making* [22]. Abstraction allows us to extend a concept to novel situations. It is also driven by analogy-making, which maps the current situation to the previous experience stored in the memory. Indeed, analogy-making has been argued to be one of the most important abilities of human cognition, or even further, “a concept is a package of analogies” [12]. The ability for humans to traverse seamlessly across concrete and abstraction levels suggests another mechanism known as *indirection* to bind two representations and use one representation to refer to the other [16, 20].

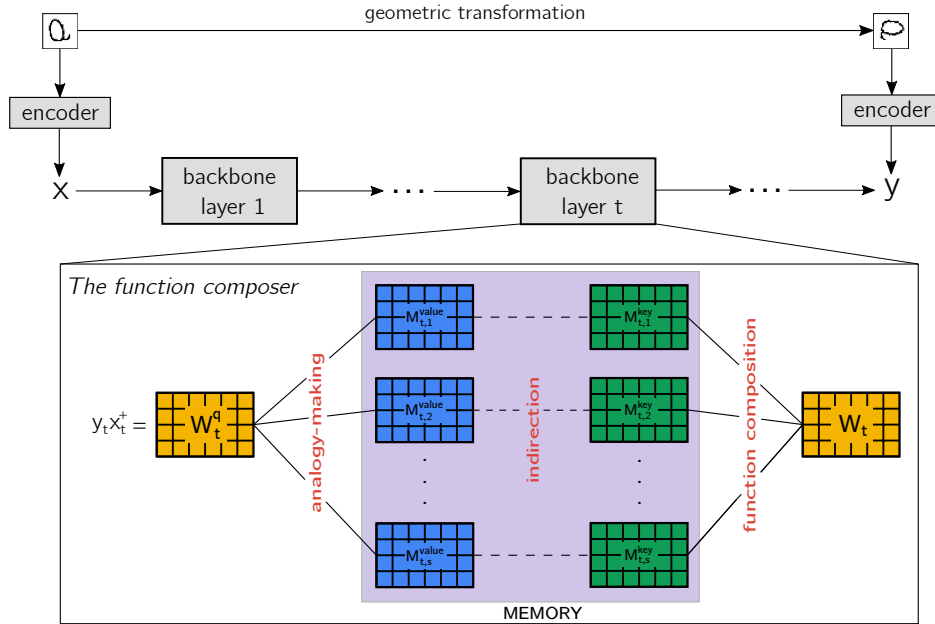


Figure 1: FINE architecture. *Above*: FINE uses a pre-defined deep backbone architecture to approximate a function mapping a given input embedding  $x$  to a given output embedding  $y$ . *Below*: given the input  $x_t$  and pseudo-output  $y_t$  of the  $t^{\text{th}}$  backbone layer, FINE first computes the query  $W_t^q$  which represents the relation between  $x_t$  and  $y_t$ . Then FINE performs analogy-making to compare the query with past experiences in the form of value memories. Finally, FINE binds the value memories with associated key memories via indirection and computes the weight  $W_t$  for the  $t^{\text{th}}$  backbone layer.

Several deep learning models have successfully utilized analogy and indirection. The Transformer [30] and RelationNet [28] learn analogies between data, through self-attention or pairwise functions. The ESN [33] goes further by incorporating the indirection mechanism to bind an entity to a symbol and then reason on the symbols; and this has proved to be efficient on tasks involving abstract rules, similar to those aforementioned IQ tests. However, a common drawback of these approaches is that they operate on the data space, and thus are susceptible to out-of-distribution samples.

In this paper, we propose to perform analogy-making and indirection in *functional* spaces instead. We aim to *learn to compose* a functional mapping from a given input to an output *on-the-fly*. By doing so, we achieve two clear advantages. First, since the class of possible mappings is often restricted, it may not require a large amount of training data to learn the distribution of functions. Second, more importantly, since this approach performs indirection in functional spaces, it avoids bindings between numerous entities and symbols in data spaces, thus may help improve the out-of-distribution generalization capability.

To this end, we introduce a new class of problems that requires functional analogy-making and indirection, which are deemed to be challenging for current data-oriented approaches. The tasks are similar to popular IQ tasks in which the model is given hints about the hidden rules, then it has to predict the missing answer following the rules. One reasonable approach is that models should be able to compare the current task to what they saw previously to identify the rules between appearing entities, and thus has to search on functional spaces instead of data spaces. More concretely, we construct the IQ tasks by applying geometric transformations to images from MNIST dataset, handwritten Omniglot dataset and real-image CIFAR100 dataset, where the training set and test set contain disjoint image classes from the same or different datasets, and possibly disjoint transformation rules.

Second, we present a novel framework named Functional Indirection Neural Estimator (FINE) to solve this class of problems (see Fig. 1 for the overall architecture of FINE). FINE consists of (a) a neural backbone to approximate the functions and (b) a trainable key-value memory module that stores the basis of the network weights that spans the space of possible functions defined by the backbone. The weight basis memories allow FINE to perform analogy-making and indirection in the function space. More concretely, when a new IQ task arrives, FINE first (1) takes the hint images to make analogies with value memories, then (2) performs indirection to bind value memories with key memories and finally (3) computes the approximated functions based on key memories. Throughout

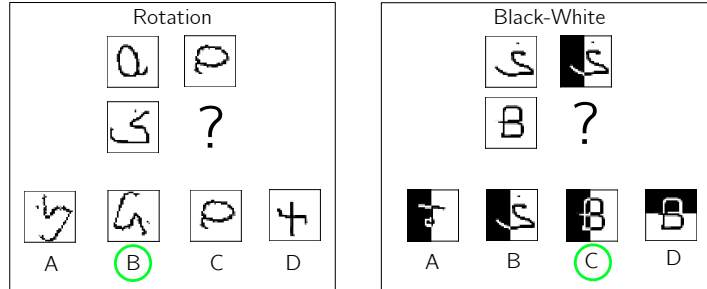


Figure 2: Examples of two IQ tasks involving geometric transformations. Choices with green circles are the correct solutions. *Left.* 90-degree rotation. *Right.* syntactic black-white transformation: a part of the image is transformed to the opposite colors.

a comprehensive suite of experiments, we demonstrate that FINE outperforms the competing methods and adapts more effectively in small data scenarios.

## 2 Tasks

For concreteness, we will focus on Intelligence Quotient (IQ) tests, which have been widely accepted as one of the reliable benchmarks to measure human intelligence [26]. We will study a popular class of IQ tasks that provides hints following some hidden rules and requires the player to choose among given choices to fill in a placeholder so that the filled-in entity obeys the rules of the current task. In order to succeed in these tasks, the player must be able to figure out the hidden rules and perform analogy-making to select the correct choice. Moreover, once figuring out the rules for the current task, a human player can almost always solve tasks with similar rules regardless of the appearing entities given in the tasks. This remarkable ability of out-of-distribution generalization indicates that humans treat objects and relations abstractly instead of relying on the raw sensory data.

We aim to solve IQ tasks that involve geometric transformations (e.g., see Fig. 2 for an example), which include affine transformations (translation, rotation, shear, scale, and reflection), non-linear transformations (fisheye, horizontal wave) and syntactic transformations (black-white, swap). Details of transformations are given in Supplementary. In a task, the models are given 3 images  $x, y$  and  $x'$ , where  $y$  is the result of  $x$  after applying a geometric transformation. The models are then asked to select  $y'$  among 4 choices  $y_1, y_2, y_3, y_4$  so that  $(x', y')$  follows the same rule as  $(x, y)$  (i.e. if  $y = f(x)$  then  $y' = f(x')$  for transformation  $f$ ). The 4 choices include (i) one with correct object/image and correct transformation (which is the solution), (ii) one with correct object/image and incorrect transformation, (iii) one with incorrect object/image and correct transformation, and (iv) one with both incorrect object/image and transformation.

Inspired by human capability, a reasonable approach to solve these tasks is that models should be able to figure out the transformation (or relation) between objects/images and apply the transformation to novel objects/images. The datasets can be classified into two main categories: single-transformation datasets and multi-transformation datasets. Single-transformation datasets are ones that only include a particular transformation, e.g. rotation. Note that the individual transformations of the same type vary, e.g., rotations by different angles. Multi-transformation datasets, on the other hand, consist of several transformation types. To test the generalization capability of the models, we build testing sets including classes of images that have never been seen during training (see Section 4.1 and Section 4.2), or even more challenging tasks including unseen rules and unseen datasets (see Section 4.3). Models must be able to leverage knowledge and memory gained from the training dataset to solve a new task.

## 3 Method

### 3.1 Functional Hypothesis

Let  $\mathcal{X}$  and  $\mathcal{Y}$  be the data input and output spaces, respectively. Denote by  $(\mathcal{X}_{\text{train}}, \mathcal{Y}_{\text{train}}) \subset (\mathcal{X}, \mathcal{Y})$  the training set, and  $(\mathcal{X}_{\text{test}}, \mathcal{Y}_{\text{test}}) \subset (\mathcal{X}, \mathcal{Y})$  the non-overlapping test set. Classical ML assumes that  $\mathcal{X}_{\text{train}}$  and  $\mathcal{X}_{\text{test}}$  are drawn from the same distribution. Under this hypothesis, it is reasonable (for frequentists) to find a function  $f: \mathcal{X} \rightarrow \mathcal{Y}$  in the functional space  $\mathcal{F}$  that fits both the train and the test

sets (i.e., the discrepancy between  $f(x)$  and corresponding  $y$  is small for all  $(x, y)$  in  $(\mathcal{X}_{\text{train}}, \mathcal{Y}_{\text{train}})$  and  $(\mathcal{X}_{\text{test}}, \mathcal{Y}_{\text{test}})$ ). However, when  $\mathcal{X}_{\text{test}}$  is drawn from a different data distribution from that of  $\mathcal{X}_{\text{train}}$ , it has been widely reported that current deep learning models fail drastically [2, 8, 13, 32, 33]. This is because the models are inferred exclusively from the observed data distribution. Moreover, it could be the case that relations between  $x$  and  $y$  in testing samples are unseen during training, which raises questions on the feasibility of learning a single function when dealing with out-of-distribution tasks. A natural solution for this problem would be to train the model to learn the functions adaptively. Formally speaking, the model will learn a *function composer*  $\phi: \mathcal{X} \times \mathcal{Y} \rightarrow \mathcal{F}$  that maps each pair of  $(x, y) \in \mathcal{X} \times \mathcal{Y}$  (where  $y$  is the associated output of  $x$ ) to a function  $\phi_{x,y}$  in  $\mathcal{F}$  so that  $\phi_{x,y}$  approximates the true relation between  $x$  and  $y$ . As discussed, training models this way leads to two clear advantages: (1) it can help to handle the cases when there are multiple (and possibly disjoint) relations between inputs and outputs within the training and testing datasets; and (2) models are less dependent on data and thus can achieve more stable results on different training and testing sets. Empirical evidence for these points will be given in Section 4.

Since there are an infinite number of functions that can map an input to an output with any given degree of precision, the key is to design  $\phi$  so that it can map a given input-output pair to a “good enough” function. We humans may draw analogies between the current situation and our experiences and then work out the most suitable options [12]. For example, we can recognize a math problem in exam to be similar to a previous exercise in class with different variable names. We may find the presented idea in a paper related to that in another paper we read before, as someone even says “new ideas are just re-distribution of old ideas”. All these examples illustrate that analogy-making is a powerful strategy in human thinking process. Inspired by this mechanism, we equip the function composer  $\phi$  with a semantic memory to store past knowledge, on which analogy-making is performed. The memory also plays the role of constraining the searching region for  $\phi$ , so that  $\phi$  only looks for functions in the subspaces spanned by the memories instead of the whole functional space  $\mathcal{F}$ . Further analysis is given in Supplementary.

A remaining question is how to design the memory. Let us be inspired again by human thinking process: When we see an animal, we compare its face, legs or tail with things we know and finally conclude it’s a “dog”. Here “dog” is an abstract concept bound with primary characteristics (e.g. face, legs, tail, etc.); once a new entity arrives, we compare its properties with these characteristics, and if they are similar, we utilize the indirection mechanism to infer it is indeed the concept we are considering. In our case, the concepts are functions, or more specifically, the geometric transformations. We thus maintain a key-value memory structure, in which the keys represent abstract concepts and values the associated characteristics of the concepts. A new input-output pair matches with some values, and the indirection enables us to compute the functions based on corresponding keys.

Note that we have swapped the role of keys and values of the traditional memory (where the query is matched against the key, not value). This is to emphasize that we perform indirection to map concrete functional values to abstract functional keys.

### 3.2 Functional Indirection Neural Estimator

In this section, we present the Functional Indirection Neural Estimator (FINE), an neural architecture to realize the general idea laid out in Section 3.1. FINE learns to compose a function mapping an input embedding  $x$  to an output embedding  $y$  on-the-fly. The function is drawn from a parametric family specified by a backbone neural network. Coupled with the backbone is a *function composer*  $\phi$ , which is trained to compute the parameters of the backbone. More specifically,  $\phi$  maps a data input-output pair to the weights of the neural networks.

FINE solves the proposed IQ tasks as follows: (1) Given two images  $x, y$  from the hint, FINE uses  $\phi$  to produce the function transforming  $x$  to  $y$ ; denoted by  $\phi_{x,y}$ . (2) Then, we feed the third image  $x'$  to  $\phi_{x,y}$  and get output  $y^* = \phi_{x,y}(x')$ . (3) We define a *similarity metric* to compare  $y^*$  with given choices. The choice with the closest distance from  $y^*$  is model’s answer. The function composer and the similarity metric are specified as follows.

**Encoder:** Images are encoded by a trainable encoder (see Fig. 1). To effectively solve IQ tasks introduced in Section 2, we use the  $p4$ -CNN [7] encoder to serve as an inductive bias for geometric transformations. Throughout this paper, we refer to the images by their embeddings.

## The functional memory

Let us focus a weight matrix  $W_t \in \mathbb{R}^{d_t^{\text{in}} \times d_t^{\text{out}}}$  at the  $t$ -th layer of the backbone network. In practice,  $W_t$  belongs to the huge  $d_t^{\text{in}} \times d_t^{\text{out}}$ -dimensional real matrix space  $\mathcal{M}_{d_t^{\text{in}}, d_t^{\text{out}}}$ . To reduce the complexity of  $W_t$ , we assume that  $W_t$  only belongs to a  $s$ -dimensional subspace of  $\mathcal{M}_{d_t^{\text{in}}, d_t^{\text{out}}}$ , where  $s \ll d_t^{\text{in}} d_t^{\text{out}}$ . This subspace has a basis of  $s$  matrices which are trainable and stored in FINE’s memory, and  $W_t$  will be written as a linear combination of these matrices.

Denote by  $M_t$  the memory for the  $t$ -th backbone layer.  $M_t$  includes two sub-memories: the key memory  $M_t^{\text{key}} = \{M_{t,1}^{\text{key}}, \dots, M_{t,s}^{\text{key}}\}$  and the corresponding value memory  $M_t^{\text{value}} = \{M_{t,1}^{\text{value}}, \dots, M_{t,s}^{\text{value}}\}$ . Elements of  $M_t^{\text{key}}$  and  $M_t^{\text{value}}$  are trainable matrices of size  $d_t^{\text{in}} \times d_t^{\text{out}}$ . We further let  $x_t \in \mathbb{R}^{d_t^{\text{in}}}$  and  $y_t \in \mathbb{R}^{d_t^{\text{out}}}$  be the associated input and output, respectively, where  $x_t$  is output of the  $(t-1)$ -th layer and  $y_t$  is the pseudo-output computed by a trainable 1-layer neural network  $y_t = \gamma_t(y)$ .

With this design, we control the complexity of functional hypothesis space by either constraining the form of the backbone or the capacity of the functional memory.

## Memory reading

By the virtue of simplicity, we aim to find a simple query that can demonstrate the relation between  $x_t$  and  $y_t$ . Although the exact relation may be non-linear, we found that a query induced from linear relation is enough to efficiently read from memory. Formally, we want to find a query  $W_t^q$  such that  $W_t^q x_t = y_t$ . The best-approximated solution is  $W_t^q = y_t x_t^\dagger$ , where  $x_t^\dagger$  is the pseudo-inverse of  $x_t$  and can be efficiently approximated by the iterative Ben-Israel and Cohen algorithm [3]. This way of query computing requires no parameter as opposed to other methods, where the input is often fed into a trainable neural network to compute the query.

With the query in hand, the next step is to perform analogy-making. In FINE, the query  $W_t^q$  represents for the current situation and the value memory  $M_t^{\text{value}}$  consists of past experiences. The concrete query interacts with value memories to measure how close the current situation is to each of the experiences. The similarities are computed as dot products between the query and value memories and normalized by a factor of  $\sqrt{d_t^{\text{in}} d_t^{\text{out}}}$ :

$$a_t = \frac{\text{fconcat}(M_t^{\text{value}})^\top \cdot \text{flatten}(W_t^q)}{\sqrt{d_t^{\text{in}} d_t^{\text{out}}}}, \quad (1)$$

where the `flatten` operator flattens the matrix  $W_t^q$  of size  $d_t^{\text{in}} \times d_t^{\text{out}}$  into a vector of size  $d_t^{\text{in}} d_t^{\text{out}}$ , while the `fconcat` operator first flattens all matrices in  $M_t^{\text{value}}$ , then concatenates them together to form the value matrix of size  $(d_t^{\text{in}} d_t^{\text{out}}) \times s$ . The resulting  $a_t$  is a  $s$ -dimensional vector measuring the similarities between the query and the entries in the value memory. Here we omit the softmax operator as in usual attention to allow the similarities with more freedom. The same idea is shared in the ESN [33], where the softmax similarities are scaled by a sigmoidal factor.

Finally, the value memories are bound with their associated key memories via indirection. This can be understood as moving forward from the concrete space of data and value memories to the abstract space of functions and key memories. With the key memories and the similarity vector  $a_t$ , the weight  $W_t$  of current backbone layer can be computed as the linear combination of key memories:

$$W_t = \text{reshape} \left( \text{fconcat}(M_t^{\text{key}}) \cdot a_t \right), \quad (2)$$

where the `reshape` operator reshapes the vector of size  $d_t^{\text{in}} d_t^{\text{out}}$  to a matrix of size  $d_t^{\text{in}} \times d_t^{\text{out}}$ . Since the softmax is omitted when calculating the similarities,  $W_t$  is not constrained to be in the convex hull of the key memories and indeed can lie anywhere in the subspace spanned by those key memories.

## Memory update

The key and value memories are updated using gradient descent:

$$M_{t,i}^{\text{key/value}} \leftarrow M_{t,i}^{\text{key/value}} - \lambda \frac{\partial L}{\partial M_{t,i}^{\text{key/value}}}, \quad \forall i = 1, 2, \dots, s, \quad (3)$$

where  $\lambda > 0$  is the learning rate and  $L$  is the loss of the training step.

### The similarity metric

After determining  $\phi_{x,y}$ , the model is given a new input  $x'$  and being asked to select the correct associated output  $y'$  among 4 choices  $y'_1, y'_2, y'_3, y'_4$  so that  $(x', y')$  follows the same transformation rule as  $(x, y)$ . This problem can be cast as finding the choice that is the most similar with  $y^* = \phi_{x,y}(x')$ . We consider the weighted Euclidean metric that measures the distance between two vectors  $u, v \in \mathbb{R}^d$ :

$$\eta(u, v) = \sum_{i=1}^d \alpha_i (u_i - v_i)^2,$$

where  $\{\alpha_i\}_{i=1}^d \geq 0$  are trainable scalars, i.e., each component of  $u$  and  $v$  contributes with different importance. Finally, the probability to pick a choice is computed as:

$$p(y'_i | x') = \frac{\exp(-\eta(y'_i, y^*))}{\sum_{j=1}^4 \exp(-\eta(y'_j, y^*))}, \quad \text{for } i = 1, 2, 3, 4.$$

## 4 Experiments

We conduct experiments to show the out-of-distribution generalization capability of FINE when performing tasks introduced in Section 2. For non-invertible transformations (e.g. reflection), we use a simple 2-layer MLP as the backbone. For invertible transformations, we use the NICE architecture [9] as backbone to serve as an inductive bias for invertibility. Since in each NICE layer, only half of the input is transformed, we use the same memory for two consecutive layers, i.e.,  $M_{2t} = M_{2t+1}$ . To balance between the backbone complexity and computational cost, we use 4 NICE layers in all experiments.

We compare FINE with three major classes of models: (a) models that make analogies in the data space, including Transformer [30], PrediNet [29] and RelationNet [28]; (b) models that leverage indirection to bind feature vectors with associated symbols and reason on the symbols, including the ESNB [33]; and (c) models that aim to learn a mapping from data to the functional space, including the HyperNetworks [14]. For HyperNetworks, we still use the NICE backbone and just apply their fast-weight generation method for fair comparisons. Except for FINE and HyperNetworks, all models are trained with context normalization [32], which has been proved to be effective in improving the generalization ability.

**Datasets & implementation:** We generate data for IQ tasks described in Section 2 using images from Omniglot dataset [5], which includes 1,623 handwritten characters, and real-image CIFAR100 dataset [17]. If not specified, models are trained with  $p4$ -CNN encoder [7]. Experiments are conducted using PyTorch on a single GPU with Adam optimizer. Reported results are averages of 10 runs.

### 4.1 Results on Omniglot Dataset

	Single-transformation									Multi affine
	Affine					Non-linear		Syntactic		
	Trans.	Rot.	Refl.	Shear	Scale	Fish.	H.Wave	B&W	Swap	
RelationNet	27.1	26.2	25.5	27	27.5	26.1	30.2	49.7	26.0	25.3
PrediNet	68.5	43.9	32.9	62.4	65.7	36.2	46.1	60.5	57.5	34.9
HyperNet	88.9	62.0	94.0	74.5	81.8	63.2	80.4	88.6	90.1	54.0
Transformer	89.5	64.8	44.3	86.3	84.0	41.4	91.0	97.6	49.9	59.4
ESBN	79.8	58.6	50.1	84.5	83.4	67.1	86.4	90.5	71.6	63.1
FINE-MLP	<b>96.1</b>	73.9	<b>95.1</b>	84.5	86.0	70.4	84.8	94.9	87.5	<b>72.0</b>
FINE-NICE	94.3	<b>77.6</b>	57.7	<b>87.2</b>	<b>86.6</b>	<b>78.5</b>	<b>95.9</b>	<b>98.4</b>	<b>96.2</b>	69.1

Table 1: Test accuracy (%) on Omniglot dataset.

We use 100 characters for training and other 800 characters for testing. The train and test set size is 10,000 and 20,000, respectively. For FINE, we use 4 NICE layers with 48 memories for each pair

of NICE layers. Experimental results for single-transformation tasks are shown in Table 1. Overall, FINE dominates others with large margins. For example, the gap to the runner-up on the Rotation task is nearly 13%. With test accuracy over 75% on all tasks, FINE shows a strong capability of out-of-distribution generalization.

We further conduct multi-affine-transformation experiments. In this case, the training set includes multiple types of affine transformations, while other settings are similar to the single-transformation case. Results are also reported in Table 1. FINE continues to outperform other models. This is because only FINE explicitly assumes the existence of multiple good functions that represent the transformation from input to output data. We note that although HyperNet also makes a similar assumption by generating data-specific weights, it does not utilize analogy-making and indirection and thus, fails to generalize to unseen images.

## 4.2 Results on CIFAR100 Dataset

	Affine					Non-linear		Syntactic	
	Trans.	Rot.	Refl.	Shear	Scale	Fish.	H.Wave	B&W	Swap
RelationNet	59.9	49.6	29.9	45.3	66.2	28.7	39.5	26.2	29.7
PrediNet	72.4	65.6	40.6	74.3	76.1	37.1	53.9	32.7	39.6
HyperNet	94.8	86.8	46.6	91.3	85.2	46.8	80.5	47.8	46.0
Transformer	98.4	86.3	47.5	95.4	84.9	47.2	95.1	51.6	47.6
ESBN	96.6	81.9	50.6	90.1	81.5	57.7	95.7	68.8	50.5
FINE-MLP	98.9	89.7	<b>80.6</b>	<b>95.7</b>	86.8	59.6	95.2	83.1	50.8
FINE-NICE	<b>99.2</b>	<b>91.3</b>	51.1	95.6	<b>87.0</b>	<b>76.8</b>	<b>98.3</b>	<b>89.1</b>	<b>51.6</b>

Table 2: Test accuracy (%) on CIFAR100 dataset of single-transformation tasks. For readability we report only the mean values here. Full table is reported in Supplementary.

	RelationNet	PrediNet	Transformer	ESBN	FINE -MLP	FINE -NICE
Group CNN	32.5 ± 1.1	46 ± 1.0	67.8 ± 4.5	71.1 ± 0.5	79.6 ± 0.5	<b>81.6 ± 0.5</b>
3-layer ResNet	31.1 ± 2.7	55.9 ± 1.7	28.5 ± 0.5	66.8 ± 9.7	<b>77.8 ± 0.5</b>	73.5 ± 1.6
MLP	47.2 ± 2.6	59.3 ± 0.8	61.5 ± 1.4	54.7 ± 2.6	<b>72.9 ± 1.1</b>	70.0 ± 1.3

Table 3: Test accuracy (%) on CIFAR100 dataset of multi-affine-transformation tasks.

For CIFAR100 dataset, we follow similar settings as in experiments on the Omniglot dataset, except that we use 50 classes for training and 50 remaining classes for testing. We also conduct experiments on single-transformation and multi-affine-transformation tasks. Results for single-transformation tasks are reported in Table 2. Again, FINE outperforms all other models on all tasks, especially on Reflection where the gap is nearly 30%. Although FINE does not show good performance on Swap task as in Omniglot experiments, it is still slightly better than other models. On the remaining tasks, FINE achieves test accuracy of more than 80%.

For the multi-affine-transformation task, we report the performances of the models when trained with different encoder architectures, including the  $p4$ -CNN, 3-layer ResNet and 2-layer MLP, in Table 3. The results show two superior characteristics of FINE: first, FINE is consistently better than other models across different encoders; second, FINE is more stable with small standard deviations. This empirical result supports the functional hypothesis stated in Section 3.1, where we suggest that focusing on functions distribution instead of data distribution can boost model’s generalization capability and stability.

## 4.3 More Extreme OOD Tasks

Previous tasks only include unseen classes of objects during testing. In this section, we further test FINE and related models on more challenging OOD tasks: tasks with unseen rules during training and even ones with images from unseen datasets. The training and testing sets are either images from CIFAR100, Omniglot or MNIST datasets, while the hidden rules are either translation, rotation or shear. For translation, training problems consist of translation vectors  $(a, b)$  with  $|a|, |b| \leq 3$ ,

Train set Test set	CIFAR 100			CIFAR100 Omniglot			Omniglot MNIST		
	Trans.	Rot.	Shear	Trans.	Rot.	Shear	Trans.	Rot.	Shear
RelationNet	25.4	26.5	26.4	25	24.9	25	24.8	25	25.2
PrediNet	25.5	39.4	36.2	26.2	26.1	26.3	23.8	26.4	25.8
HyperNet	31.6	67.2	58.6	22.2	26.4	22.9	22.7	29	28.2
Transformer	30.9	64.2	55	<b>30</b>	31.7	33.8	28.4	27	25.1
ESBN	16.4	81.3	42.8	15.4	39.2	33.3	17.7	41.3	36.6
<b>FINE</b>	<b>62</b>	<b>85.6</b>	<b>77.8</b>	22.1	<b>43.2</b>	<b>39.2</b>	<b>39.4</b>	<b>44.7</b>	<b>37.9</b>

Table 4: Test accuracy (%) on more extreme OOD tasks with unseen objects, unseen rules and (possibly) unseen datasets. *Translation*: train with translation vectors  $(a, b)$  with  $|a|, |b| \leq 3$ , test with either  $|a| > 3$  or  $|b| > 3$ . *Rotation*: train with rotation angles  $\alpha \leq 180^\circ$ , test with  $\alpha > 180^\circ$ . *Shear*: train with shear angles  $(\alpha, \beta)$  with  $|\alpha|, |\beta| \leq 30^\circ$ , test with either  $|\alpha| > 30^\circ$  or  $|\beta| > 30^\circ$ .

and models are tested with either  $|a| > 3$  or  $|b| > 3$ ; for rotation, model are trained with angles  $\alpha \leq 180^\circ$  and tested with  $\alpha > 180^\circ$ ; for shear, training angles  $(\alpha, \beta)$  are ones with  $|\alpha|, |\beta| \leq 30^\circ$ , while testing ones are either  $|\alpha| > 30^\circ$  or  $|\beta| > 30^\circ$ . All tasks have 5,000 data points for training and 10,000 for testing. We report results of FINE with NICE backbone and related models in Table 4. As expected, FINE continues to outperform other models on most of the tasks, even on extreme OOD tasks with unseen datasets and unseen rules where performances of all models drop significantly. This demonstrates FINE is capable of effectively learning the basis weights, which are stored in the memory, to represent novel rules.

#### 4.4 Model Analysis and Ablation Study

##### Clustering on functional spaces

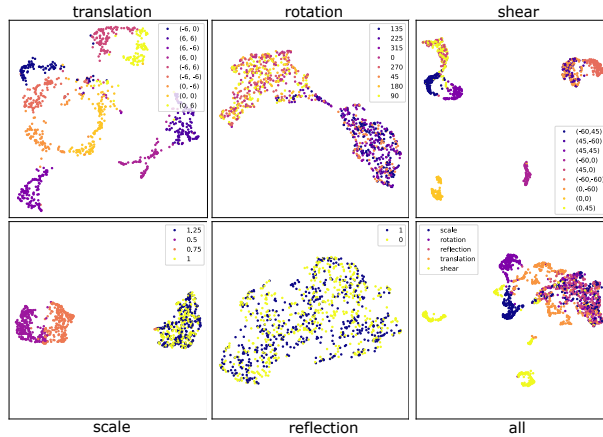


Figure 3: *Clusters on functional space*. We project weights produced by the function composer  $\phi$  to see whether  $\phi_{x_1, y_1}$  locates closely to  $\phi_{x_2, y_2}$  on the functional space if the relation between  $x_1$  and  $y_1$  is similar to that between  $x_2$  and  $y_2$ . Except for Reflection, the weights are nicely clustered.

We study how the transformations are distributed in the functional space. We use the FINE model trained on multi-affine transformation tasks. For an input-output pair  $(x, y)$ , we flatten and concatenate all weights of NICE layers to form a vector representing  $\phi_{x, y}$ . We then use the UMAP [21] to project  $\phi_{x, y}$ 's vectors onto the 2D plane. Results are shown in Fig. 3. It is interesting to see that shears with the same horizontal or vertical angles are positioned closely; and scales are separated into 2 “big” clusters, one for smaller scale and one for bigger scale. In contrast, reflection representations seem not to be clustered properly, which is worth further investigation in future work.

##### Number of memories and backbone layers

We do an ablation study to see the effect of number of memories and backbone layers in FINE. For the limit case with 0 memory, we assign the query matrices to be the weights for NICE layers without



the analogy-making and indirection process. For the limit case with 0 NICE layer, we replace the NICE backbone by a 2-layer MLP.

Results are shown in Fig. 4(a). Overall, we can observe clear improvements when we increase the number of memories or number of NICE layers. More interestingly, the more number of memories is, the more stable the results will be. Increasing the number of memories is equivalent to enlarging the range of  $\phi$ , and increasing the number of NICE layers is equivalent to enlarging the hypothesis space  $\mathcal{F}$ . Enlarging  $\mathcal{F}$  may help FINE approach the true functions while still being sufficiently constrained by the number of memories, thus still being able to maintain its generalization capability.

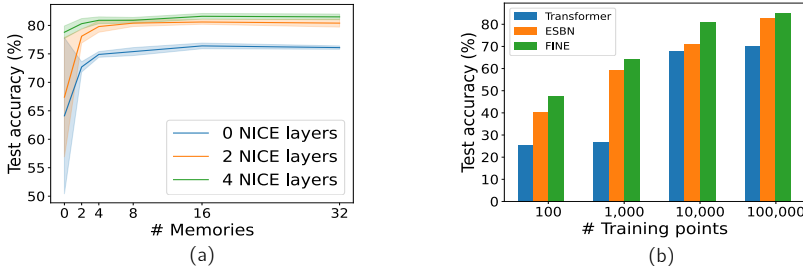


Figure 4: (a) Performance of FINE with different number of memories and backbone layers. Overall, the test accuracy increases with more memories and backbone layers. (b) Performance with different number of training points. FINE works fairly well on small datasets while others may fail significantly.

### Number of training data points

We train models on multi-affine-transformation task with training sets of different sizes. Results are reported in Fig. 4(b). FINE can adapt with small datasets of sizes 100 or 1000 and achieve fair accuracy (47.8% and 64.4%, respectively). Moreover, FINE achieves average test accuracy of 81.1% on training set of size 10,000, which is quite close to the 85.3% accuracy on 100,000 data points training sets. This shows FINE may obtain a near-optimal solution even with small number of training data points. In contrast, ESNB and Transformer need 100,000 training data points to achieve 80% or higher test accuracy, while only achieving roughly 70% test accuracy on smaller datasets.

## 5 Related work

In recent years, there has been a strong interest in designing models that are capable of generalizing systematically. The Module Networks [1], which dynamically compose neural networks out of trainable modules, have been shown to possess some degree of systematic generalization [2]. Parascandolo et al. [24] proposed a method to train multiple competing experts to explain image transformations on MNIST and Omniglot datasets, yet the transformations are simpler than ones in our FINE dataset and it is not clear whether the proposed method can deal with unseen transformations. The Neural Interpreter [25] uses attention mechanism to recombine functional modules for each input-output pair and test their method on abstract reasoning tasks, yet tends to require a large amount of data to learn. Switch Transformer [10] mitigates the communication and computational cost in mixture of experts models. Recently, ESNB [33], which utilizes the indirection mechanism, shows a great promise on OOD tasks. Both methods achieve their degree of systematic generalization by injecting symbolic biases into the models. Our model FINE follows the same strategy, but it performs analogy-making and indirection in functional spaces instead of data spaces, and this has proved to boost both the performance and stability.

IQ tests are powerful testbeds for visual and abstract reasoning. Inspired by Raven’s Progressive Matrices (RPM), the RAVEN dataset [34] was proposed as a testbed for visual reasoning models. However, this dataset does not focus on testing the ability of OOD generalization. Webb et al. [33] propose a series of IQ tasks with Unicode characters to show the effectiveness of indirection in tasks involving abstract rules, however these tasks are relatively simple since they only require the models to understand the same-different relation. The ARC dataset [6] aims to serve as a benchmark for general intelligence and includes various psychometric IQ tasks in the form of grid structures. In this paper, we propose IQ tasks involving geometric transformations as introduced in Section 2. These tasks are not only flexible so that we can include images from different datasets or create/combine numerous transformations, but also challenging to test OOD generalization abilities of models.

The weight composition feature of FINE links back to the concept of fast weights [19], the idea of computing data-specific network weights on-the-fly. HyperNetworks [14] stylizes this idea by computing the fast weights using a separate trainable (slow weight) network. The Meta-learned Neural Memory [23] uses the pseudo-target technique (which we also leverage in FINE) and appropriately updates the short-term memory once new input arrives. The Neural Stored-Program Memory (NSM) [18] proposes a hybrid approach between slow-weight and fast-weight to compute network weights on-the-fly based on slow-weight key and value memories. However, NSM only performs on sequential learning tasks, while FINE aims to solve OOD IQ tasks requiring abstract cognition. Moreover, FINE computes the query based on the input and the (pseudo-) output, while NSM’s query is computed based on the input only. Memories have been to be versatile in meta-learning and few-shot learning [15, 27, 31] due to the ability to rapidly store past examples and adapt to new situations. In our case, an IQ task can be thought of as a one-shot learning scenario in which FINE has to make use of the long-term key-value memory to adapt to the current task.

## 6 Limitations

Operating in functional spaces requires FINE’s memory to store several trainable weight matrices to infer the data-specific weights for the backbone. Moreover, each layer of the backbone requires its own memory, thus FINE may need a large number of parameters for very deep backbones. This could be addressed by parameter-sharing across layers and limiting the rank of the weight matrices.

It remains to design the backbone architecture optimally. We have used the NICE architecture as backbone for invertible transformations and a 2-layer MLP backbone for non-invertible cases. We further investigated our model’s performances with larger number of training points (up to 1M) and observed that FINE with the NICE backbone peaks at 100,000 training points with around 85% test accuracy, while FINE with MLP backbone continues to improve and achieves around 95% test accuracy at 1M training points. This calls for further theoretical analysis to guide the architectural design of the backbone network.

Finally, testing FINE on IQ tasks in the visual space may limit its potential on IQ tasks involving other modalities. For example, one may consider a textual IQ problem: “if  $abc \rightarrow abd$ , then  $mmnpp \rightarrow ?$ ”. It is worth to emphasize that the concepts of analogy-making and indirection in functional spaces are indeed general and thus the idea of FINE should be applicable to various scenarios.

## 7 Conclusion

To study the out-of-distribution (OOD) generalization capability of models, we have proposed IQ tasks that require models to rapidly recognize the hidden rules of geometric transformations between a pair of images and transfer the rules to a new pair of different image classes. Such tasks would necessitate human-like abilities for conceptual abstraction, analogy-making, and utilizing indirection. We put forward a hypothesis that these mechanisms should be performed in the functional space instead of data space as in current deep learning models. To realize the hypothesis, we then proposed FINE, a memory-augmented neural architecture that learns to compose functions mapping an input to an output on-the-fly. The memory has two trainable components: the value sub-memory and the binding key sub-memory, where the keys are basis weight matrices that span the space of functions. For an IQ task, when given a hint in the form of an input-output pair, and FINE estimates the analogy between the pair and the values as mixing coefficients. These coefficients are then used to mix the binding keys via indirection to generate the weights of the backbone neural net which computes the intended function. For a test input of different class, the function is used to estimate the most compatible output, thus solving the IO task. Through an extensive suite of experiments using images from the Omniglot and CIFAR100 datasets to construct the IQ tasks, FINE is found to be reliable in figuring out the hidden relational pattern in each IQ task and thus is able to solve new tasks, even with unseen image classes. Importantly, FINE outperforms other models in all experiments, and can generalize well in small data regimes.

Future works will include making FINE robust against OOD in transformations without catastrophic forgetting when new transformations are continually introduced.

## References

- [1] Jacob Andreas, Marcus Rohrbach, Trevor Darrell, and Dan Klein. Neural module networks. In *Proceedings of the IEEE conference on computer vision and pattern recognition*, pages 39–48, 2016.
- [2] Dzmitry Bahdanau, Shikhar Murty, Michael Noukhovitch, Thien Huu Nguyen, Harm de Vries, and Aaron Courville. Systematic generalization: What is required and can it be learned? In *International Conference on Learning Representations*, 2018.
- [3] A. Ben-Israel and D. Cohen. On iterative computation of generalized inverses and associated projections. *SIAM Journal on Numerical Analysis*, 3:410–419, 1966.
- [4] Irving Biederman and Ginny Ju. Surface versus edge-based determinants of visual recognition. *Cognitive psychology*, 20(1):38–64, 1988.
- [5] Yuri Burda, Roger B. Grosse, and R. Salakhutdinov. Importance weighted autoencoders. *ICLR*, 2016.
- [6] François Chollet. On the measure of intelligence. *arXiv preprint arXiv:1911.01547*, 2019.
- [7] Taco Cohen and Max Welling. Group equivariant convolutional networks. In *International conference on machine learning*, pages 2990–2999. PMLR, 2016.
- [8] Róbert Csordás, Kazuki Irie, and Jürgen Schmidhuber. The devil is in the detail: Simple tricks improve systematic generalization of transformers. *arXiv preprint arXiv:2108.12284*, 2021.
- [9] Laurent Dinh, David Krueger, and Yoshua Bengio. NICE: Non-linear independent components estimation. *arXiv preprint arXiv:1410.8516*, 2014.
- [10] William Fedus, Barret Zoph, and Noam Shazeer. Switch transformers: Scaling to trillion parameter models with simple and efficient sparsity, 2021.
- [11] Robert Geirhos, Carlos RM Temme, Jonas Rauber, Heiko H Schütt, Matthias Bethge, and Felix A Wichmann. Generalisation in humans and deep neural networks. *Advances in neural information processing systems*, 31, 2018.
- [12] Dedre Gentner, Keith J Holyoak, and Boicho N Kokinov. *The analogical mind: Perspectives from cognitive science*. MIT press, 2001.
- [13] Klaus Greff, Sjoerd Van Steenkiste, and Jürgen Schmidhuber. On the binding problem in artificial neural networks. *arXiv preprint arXiv:2012.05208*, 2020.
- [14] David Ha, Andrew Dai, and Quoc V Le. Hypernetworks. *ICLR*, 2017.
- [15] Łukasz Kaiser, Ofir Nachum, Aurko Roy, and Samy Bengio. Learning to remember rare events. *ICLR*, 2017.
- [16] Trenton Kriete, David C Noelle, Jonathan D Cohen, and Randall C O’Reilly. Indirection and symbol-like processing in the prefrontal cortex and basal ganglia. *Proceedings of the National Academy of Sciences*, 110(41):16390–16395, 2013.
- [17] A. Krizhevsky. Learning multiple layers of features from tiny images. 2009.
- [18] Hung Le, Truyen Tran, and Svetha Venkatesh. Neural stored-program memory. In *ICLR 2020: Proceedings of the 8th International Conference on Learning Representations*, 2020.
- [19] Christoph von der Malsburg. The correlation theory of brain function. In *Models of neural networks*, pages 95–119. Springer, 1994.
- [20] Gary Marcus. *The algebraic mind*, 2001.
- [21] Leland McInnes, John Healy, and James Melville. Umap: Uniform manifold approximation and projection for dimension reduction. *arXiv preprint arXiv:1802.03426*, 2018.
- [22] Melanie Mitchell. Abstraction and analogy-making in artificial intelligence. *Annals of the New York Academy of Sciences*, 1505(1):79–101, 2021.
- [23] Tsendsuren Munkhdalai, Alessandro Sordoni, Tong Wang, and Adam Trischler. Metalearned neural memory. In *NeurIPS*, 2019.
- [24] Giambattista Parascandolo, Niki Kilbertus, Mateo Rojas-Carulla, and Bernhard Schölkopf. Learning independent causal mechanisms. In *International Conference on Machine Learning*, pages 4036–4044. PMLR, 2018.
- [25] Nasim Rahaman, Muhammad Waleed Gondal, Shruti Joshi, Peter Gehler, Yoshua Bengio, Francesco Locatello, and Bernhard Schölkopf. Dynamic inference with neural interpreters. *Advances in Neural Information Processing Systems*, 34:10985–10998, 2021.
- [26] Ellen W Rowe, Cristin Miller, Lauren A Ebenstein, and Dawna F Thompson. Cognitive predictors of reading and math achievement among gifted referrals. *School Psychology Quarterly*, 27(3):144, 2012.

- [27] Adam Santoro, Sergey Bartunov, Matthew Botvinick, Daan Wierstra, and Timothy Lillicrap. Meta-learning with memory-augmented neural networks. In *International conference on machine learning*, pages 1842–1850. PMLR, 2016.
- [28] Adam Santoro, David Raposo, David G Barrett, Mateusz Malinowski, Razvan Pascanu, Peter Battaglia, and Timothy Lillicrap. A simple neural network module for relational reasoning. *Advances in neural information processing systems*, 30, 2017.
- [29] Murray Shanahan, Kyriacos Nikiforou, Antonia Creswell, Christos Kaplanis, David Barrett, and Marta Garnelo. An explicitly relational neural network architecture. In *International Conference on Machine Learning*, pages 8593–8603. PMLR, 2020.
- [30] Ashish Vaswani, Noam M. Shazeer, Niki Parmar, Jakob Uszkoreit, Llion Jones, Aidan N. Gomez, Lukasz Kaiser, and Illia Polosukhin. Attention is all you need. *NeurIPS*, abs/1706.03762, 2017.
- [31] Oriol Vinyals, Charles Blundell, Timothy Lillicrap, Daan Wierstra, et al. Matching networks for one shot learning. *Advances in neural information processing systems*, 29, 2016.
- [32] Taylor Webb, Zachary Dulberg, Steven Frankland, Alexander Petrov, Randall O’Reilly, and Jonathan Cohen. Learning representations that support extrapolation. In *International conference on machine learning*, pages 10136–10146. PMLR, 2020.
- [33] Taylor Whittington Webb, Ishan Sinha, and Jonathan Cohen. Emergent symbols through binding in external memory. In *International Conference on Learning Representations*, 2020.
- [34] Chi Zhang, Feng Gao, Baoxiong Jia, Yixin Zhu, and Song-Chun Zhu. Raven: A dataset for relational and analogical visual reasoning. In *Proceedings of the IEEE Conference on Computer Vision and Pattern Recognition (CVPR)*, 2019.

## APPENDIX

### A Transformations Details

We build IQ tasks with geometric transformation of 3 categories: affine, non-linear and syntactic transformations.

#### Affine transformations

We consider 5 types of affine transformations: translation, rotation, reflection, shear, and scaling.

- *Translation*: with translation vector  $(i, j)$ , where  $i, j \in \{-9, -6, -3, 0, 3, 6, 9\}$ .
- *Rotation*: with rotation angle  $\alpha \in \{k \cdot 15^\circ : k \in \{0, 1, \dots, 23\}\}$ .
- *Reflection*: horizontal or vertical reflection.
- *Shear*: with shear angles  $(\alpha, \beta)$  where  $\alpha, \beta \in \{-60^\circ, -45^\circ, -30^\circ, -15^\circ, 0^\circ, 15^\circ, 30^\circ, 45^\circ, 60^\circ\}$ .
- *Scaling*: with scale coefficient  $s \in \{0.5, 0.75, 1, 1.25\}$ .

#### Non-linear transformations

We consider 2 types of non-linear transformations: fisheye and horizontal wave.

- *Fisheye*: given pixel  $(x, y)$ , the transformed pixel  $(T(x), T(y))$  is given by  $T(x) = x + (x - c_x) \cdot d \cdot \sqrt{(x - c_x)^2 + (y - c_y)^2}$  and  $T(y) = y + (y - c_y) \cdot d \cdot \sqrt{(x - c_x)^2 + (y - c_y)^2}$ , where  $(c_x, c_y)$  is the transformation center and  $d$  is the distortion factor.
- *Horizontal wave*: given pixel  $(x, y)$ , the transformed pixel  $(T(x), T(y))$  is given by  $T(x) = x$  and  $T(y) = y + a \cos(fy)$ , where  $a$  is the amplitude of cosine wave and  $f$  is the frequency.

#### Syntactic transformations

We consider 2 types of syntactic transformations: black-white and swap.

- *Black-white*: the image is horizontally or vertically splitted into 2 subimages (not necessarily of equal size). One subimage is kept fixed, while the other one will be transformed  $x \mapsto 1 - x$ , where  $x$  is the pixel value.
- *Swap*: the image is splitted into 4 equal subimages, which are then permuted to achieve the transformed image.

### B Principles for Designing the Hypothesis Space $\mathcal{F}$ and the Function Composer $\phi$

We aim to determine general principles for designing  $\mathcal{F}$  and  $\phi$ . Suppose  $\mu: \mathcal{X} \times \mathcal{Y} \rightarrow \mathcal{C}^0(\mathcal{X}, \mathcal{Y})$ , where  $\mathcal{C}^0(\mathcal{X}, \mathcal{Y})$  is the space of all continuous functions from  $\mathcal{X}$  to  $\mathcal{Y}$ , be the mapping that maps each input-output pair  $(x, y)$  to the correct function transforming  $x$  to  $y$ . We further define a norm  $\|\cdot\|_{\mathcal{C}^0}$  on  $\mathcal{C}^0(\mathcal{X}, \mathcal{Y})$  determined by  $\|f\|_{\mathcal{C}^0} = \sup_{x \in \mathcal{X}} \|f(x)\|_{\mathcal{Y}}$ , where  $\|\cdot\|_{\mathcal{Y}}$  is an arbitrary norm on  $\mathcal{Y}$ . Our goal is to find  $\phi$  as the solution of the optimization problem:

$$\text{Minimize } \sum_{(x,y)} \|\mu_{x,y} - \phi_{x,y}\|_{\mathcal{C}^0}. \quad (4)$$

We hypothesize that the cardinality of the range  $\mathcal{R}(\mu)$  of  $\mu$  is much less than the number of data points (i.e. the number of relations within the dataset is limited), and further suppose  $\mathcal{R}(\mu) = \{\mu_1, \mu_2, \dots, \mu_k\}$ , where  $\mu_i$ 's are functions in  $\mathcal{C}^0(\mathcal{X}, \mathcal{Y})$ . The optimization problem in Eq. ((4)) can be rewritten as:

$$\text{Minimize } \sum_{i=1}^k \sum_{(x,y): \mu_i(x)=y} \|\mu_i - \phi_{x,y}\|_{\mathcal{C}^0}. \quad (5)$$

The optimization problem in Eq. ((5)) can be deduced to multiple optimization subproblems:

$$\text{Minimize} \quad \sum_{(x,y):\mu_i(x)=y} \|\mu_i - \phi_{x,y}\|_{\mathcal{C}^0}, \quad \forall i = 1, 2, \dots, k. \quad (6)$$

For each  $i = 1, 2, \dots, k$ , let  $\phi_i^* \in \mathcal{F}$  be the function that best approximates  $\mu_i$ . By the triangle inequality, we obtain

$$\|\mu_i - \phi_{x,y}\|_{\mathcal{C}^0} \leq \|\mu_i - \phi_i^*\|_{\mathcal{C}^0} + \|\phi_i^* - \phi_{x,y}\|_{\mathcal{C}^0}, \quad \forall i = 1, 2, \dots, k.$$

Solving optimization problem Eq. ((6)) might be difficult, so we instead consider an alternative optimization problem

$$\text{Minimize} \quad \sum_{(x,y):\mu_i(x)=y} (\|\mu_i - \phi_i^*\|_{\mathcal{C}^0} + \|\phi_i^* - \phi_{x,y}\|_{\mathcal{C}^0}), \quad \forall i = 1, 2, \dots, k. \quad (7)$$

We deduce following analysis after observing Eq. ((7)):

- The term  $\|\phi_i^* - \phi_{x,y}\|_{\mathcal{C}^0}$  suggests  $\mathcal{R}(\phi)$  (the range of  $\phi$ ) should not be too small or too large, otherwise there may exist some  $(x, y)$  such that  $\phi_{x,y}$  is far away from  $\phi_i^*$ .
- Since  $\mathcal{R}(\phi)$  is constrained, so should be  $\mathcal{F}$ . If  $\mathcal{F}$  is too small,  $\|\mu_i - \phi_i^*\|_{\mathcal{C}^0}$  may be large for some  $i$ ; if  $\mathcal{F}$  is too large,  $\phi_i^*$  may be far away from  $\mathcal{R}(\phi)$ , which leads to large  $\|\phi_i^* - \phi_{x,y}\|_{\mathcal{C}^0}$ .

With the above arguments, we suggest the following principles for designing  $\mathcal{F}$  and  $\phi$ :

1.  $\mathcal{F}$  should be constrained by some prior knowledge of  $\mu$ . For example, if we know  $\mu$  is invertible, then  $\mathcal{F}$  should also contain invertible functions only.
2.  $\phi$  should be determined on the fly in a meta-learning fashion (associated with each input-output pair  $(x, y)$ ) so that we can control its complexity.

## C Training setup

For ESNB, Transformer, RelationNet and PrediNet, we follow the same settings as [33], where all given images (including examples and answer candidates) are treated as a sequence and passed through a context normalization layer before being fed to the model. For HyperNetwork, we also use the NICE backbone for fair comparisons and maintain the key memories (but not the value memories) to compute the weights; at each layer of the backbone, the attention weights are computed as the output of an LSTM cell, where the input for LSTM is the concatenation of the input and (pseudo-)output of current layer, and the hidden states are taken from the LSTM cell of previous layer. For FINE with NICE backbone, we use 4 NICE layers while using 2-layer MLP for FINE with MLP backbone. We use 8-32 basis weight matrices in the experiments.

We use the Adam optimizer with no weight decay along with gradient clipping with threshold 10 in all experiments. All tasks are trained with 200-300 epochs. The training and testing batch sizes are 32 and 100, respectively. Feature vectors of images are of size 128.

## D More Results

Table 5 reports the full result table with mean & std on Omniglot dataset of single-transformation and multi-affine-transformation task.

Table 6 reports the full result table with mean & std on CIFAR100 dataset of single-transformation tasks.

	Single-transformation									Multi affine
	Affine					Non-linear		Syntactic		
	Trans.	Rot.	Refl.	Shear	Scale	Fish.	H.Wave	B&W	Swap	
RelationNet	27.1±0.4	26.2±0.3	25.5±0.4	27±0.5	27.5±0.4	26.1±0.7	30.2±6.9	49.7±29.1	26.0±2.2	25.3±0.2
PrediNet	68.5±4.0	43.9±6.8	32.9±1.9	62.4±3.7	65.7±2.8	36.2±2.4	46.1±7.9	60.5±8.0	57.5±3.6	34.9±1.1
HyperNet	88.9±1.0	62.0±2.9	94.0±1.9	74.5±1.4	81.8±1.1	63.2±2.0	80.4±1.0	88.6±1.4	90.1±1.0	54.0±4.1
Transformer	89.5±1.0	64.8±1.5	44.3±0.9	86.3±4.1	84±0.9	41.4±11.6	91.0±11.8	97.6±0.4	49.9±18.5	59.4±6.0
ESBN	79.8±0.6	58.6±1.0	50.1±0.3	83.4±1.6	84.5±1.2	67.1±0.8	86.4±1.0	90.5±4.1	71.6±2.7	63.1±0.5
<b>FINE</b>	<b>94.3±0.4</b>	<b>77.6±0.7</b>	<b>95.1±1.0</b>	<b>87.2±0.3</b>	<b>86.6±0.4</b>	<b>78.5±0.7</b>	<b>95.9±0.4</b>	<b>98.4±0.3</b>	<b>96.2±0.2</b>	<b>69.1±0.6</b>

Table 5: Test accuracy (mean & std) (%) on Omniglot dataset.

	Affine					Non-linear		Syntactic	
	Trans.	Rot.	Refl.	Shear	Scale	Fish.	H.Wave	B&W	Swap
RelationNet	59.9±11.2	49.6±5.8	29.9±1.0	45.3±5.1	66.2±1.3	28.7±1.0	39.5±6.9	26.2±1.4	29.7±0.9
PrediNet	72.4±4.6	65.6±5.0	40.6±2.0	74.3±4.8	76.1±3.6	37.1±1.2	53.9±8.1	32.7±1.8	39.6±1.3
HyperNet	94.8±1.1	86.8±1.3	46.6±0.5	91.3±0.9	85.2±1.2	46.8±0.7	80.5±4.6	47.8±0.9	46±0.8
Transformer	98.4±1.1	86.3±3.8	47.5±1.1	95.4±1.4	84.9±1.2	47.2±1.0	95.1±1.8	51.6±14.3	47.6±0.8
ESBN	96.6±0.7	81.9±1.1	50.6±0.4	90.1±0.7	81.5±0.9	57.7±1.3	95.7±0.7	68.8±6.0	50.5±0.5
<b>FINE</b>	<b>99.2±0.1</b>	<b>91.3±0.2</b>	<b>80.6±14.5</b>	<b>95.6±0.5</b>	<b>87±0.2</b>	<b>76.8±1.3</b>	<b>98.3±0.4</b>	<b>89.1±0.7</b>	<b>51.6±1.7</b>

Table 6: Test accuracy (%) on CIFAR100 dataset of single-transformation tasks.